

Cite this article as: Li Anjin, Zhao Panchao, Yi Wei, et al. Purification and Particulate Control of Tungsten Particles by Hydrometallurgy Combined with Spray Drying-Pyrolysis Process[J]. Rare Metal Materials and Engineering, 2021, 50(04): 1241-1246.

Purification and Particulate Control of Tungsten Particles by Hydrometallurgy Combined with Spray Drying-Pyrolysis Process

Li Anjin¹, Zhao Panchao², Yi Wei¹, Xin Zena¹, Li Hongpeng¹, Pang Fangzhao¹, Li Jigang¹, Yao Chensiqi¹

¹ State Key Laboratory of Advanced Technologies for Comprehensive Utilization of Platinum Metals, Kunming Institute of Precious Metals, Kunming 650106, China; ² Northwest Institute for Non-ferrous Metal Research, Xi'an 710016, China

Abstract: high-purity well-dispersed micro-spherical W particles were synthesized by ion exchange, extraction, re-crystallization, spraying drying and pyrolysis processes with commercial ammonium paratungstate $[(\text{NH}_4)_{10}[\text{H}_2\text{W}_{12}\text{O}_{42}] \cdot n\text{H}_2\text{O}]$ as raw materials. Impurities in ammonium paratungstate were eliminated by hydrometallurgy treatment. The morphology and size of as-synthesized W particles were controlled by spraying drying-pyrolysis process. The influences of solution concentration in spray drying on the morphology of $(\text{NH}_4)_{10}[\text{H}_2\text{W}_{12}\text{O}_{42}]$ particles were investigated. The pyrolysis mechanism of spraying dried $(\text{NH}_4)_{10}[\text{H}_2\text{W}_{12}\text{O}_{42}]$ particles transformed into as-synthesized W particles was revealed. Results show that the purity of as-fabricated tungsten powder is higher than 99.995wt%, and the average size is about 1.5 μm . The size and morphology of the final particles produced can be determined by the solution concentration and velocity of the droplet generated by the atomizers. Pyrolysis temperature is one of key factors for controlling the morphology and size of as-prepared W particles. It should be noted that the hydrometallurgy and powder technology in this study can be applied to synthesize other metal particles with high-performance requirements.

Key words: high-purity; well-dispersed; micro-spherical; solution concentration; pyrolysis mechanism

Tungsten (W) is widely used as high temperature materials^[1], sputtering target materials^[2], wiring materials^[3], due to its high melting point, low sputtering yield strength and good filling properties^[4]. With the development of electronic technology, the requirement for the purity of tungsten powder is getting higher and higher^[5,6]. Electrical contact material made from high-purity tungsten powder is one of key materials of semiconductors^[7]. The purity, particle size, and morphology of tungsten powder have great influence on its properties^[6,8,9].

The current purification methods include physical purification^[10], chemical purification, solvent extraction^[11] and ion exchange^[12,13]. Compared with other methods, physical purification such as regional melting, vacuum melting, has the disadvantage of high requirements for raw materials, high cost, and time-consuming process^[14,15]. Vacuum degassing has ad-

vantages only in removing metal inclusions^[16]. There are many studies have been reported for preparing high performance tungsten particles. Kamal et al^[7] synthesized tungsten nanoparticles from heavy alloy scrap using a novel chemical route of selective precipitation and reduction. The purity of the tungsten nanoparticles is higher than 99.7wt%, and the average size of the particles decreases from 210 nm to 45 nm. It is reported that a Japanese metallurgical company developed a tungsten target with a purity of 5N in 2005, but there is few detail preparation method for this message^[17]. China patent 107470639A (Qin Mingli et al) prepared spherical tungsten powders with a narrow particle size distribution by combination of dispersion, classification and plasma spheroidization methods. All the above studies show that there are few reports referenced to the tungsten particles with high purity and suit-

Received date: April 09, 2020

Corresponding author: Li Jigang, Master, State Key Laboratory of Advanced Technologies for Comprehensive Utilization of Platinum Metals, Kunming Institute of Precious Metals, Kunming 650106, P. R. China, E-mail: lijigang@ipm.com.cn

Copyright © 2021, Northwest Institute for Nonferrous Metal Research. Published by Science Press. All rights reserved.

able properties. Therefore, the development of high purity tungsten powder with suitable particle size distribution and morphology is desired.

Spray drying method has merits of small particle size, easy control and low contamination of raw materials, so it is widely applied in medicine, food, chemical, environment protection and other fields^[18-20]. In our foregoing studies, Zhao Panchao et al used spray drying combined with two-step calcination methods to synthesize a hollow superstructure W powder using commercial $(\text{NH}_4)_{10}[\text{H}_2\text{W}_{12}\text{O}_{42}] \cdot n\text{H}_2\text{O}$ ^[16]. Bi Jun et al synthesized high-purity micro-spherical ruthenium particles by distilling, precipitation, dry spraying and ignition. The purity of the as-synthesized Ru particles is higher than 99.995%, and the average size is about 12 μm ^[21].

This study is to report a detailed investigation on the synthesis of high-purity well-dispersed micro-spherical tungsten particles by hydrometallurgy combined with spray drying-pyrolysis process. The influence mechanism of solution concentration on the spray drying process was investigated. To the best of our knowledge, there is few reports on the synthesis of purified micro-spherical W particles. A good understanding of the processing conditions is crucial to the reliability of tungsten powder and further tungsten products, and it is significant to the further development of powder fabrication technology.

1 Materials and Methods

All reagents and solvents were used as received without further purification. The purity of ammonium paratungstate was less than 98.5%, and the purity grade of other reagents including ammonium sulfide, N263, sulfonated kerosene, isooctanol was AR. High-purity N_2 (99.999%) and H_2 (99.999%) and self-made high-purity water were used in this experiment.

The $(\text{NH}_4)_{10}[\text{H}_2\text{W}_{12}\text{O}_{42}] \cdot n\text{H}_2\text{O}$ was dissolved in high-purity water at room temperature, and the solution was vulcanized to be 5 mol/L. Then, the solution flowed past the ion exchange column which mounted HBDM-1 resin and after four stages of countercurrent extraction, and the liquid flow rate was 110 mL/min. After that, the extractant system was formulated which consisted of N263 [15% (v/v)] + isooctanol [35% (v/v)] + sulfonated kerosene [50% (v/v)], O/A=1/3. The $(\text{NH}_4)_{10}[\text{H}_2\text{W}_{12}\text{O}_{42}]$ solution was purified and collected after standing still for 4 h, and then the purified $(\text{NH}_4)_{10}[\text{H}_2\text{W}_{12}\text{O}_{42}]$ sediment was obtained by evaporation crystallization.

The purified $(\text{NH}_4)_{10}[\text{H}_2\text{W}_{12}\text{O}_{42}]$ was dissolved to prepare solutions with different concentrations at different temperatures. Then, the purified micro-spherical $(\text{NH}_4)_{10}[\text{H}_2\text{W}_{12}\text{O}_{42}]$ particles were fabricated by the spray drying treatment. As-spray dried $(\text{NH}_4)_{10}[\text{H}_2\text{W}_{12}\text{O}_{42}]$ particles were calcined in N_2/H_2 (v/v 3:1) at different temperatures (600, 650, 700, 750 °C) for 2 h and cooled under N_2/H_2 . Finally, the purified micro-spherical tungsten particles were synthesized.

Self-made ion exchange device and extraction unit were used to purify $(\text{NH}_4)_{10}[\text{H}_2\text{W}_{12}\text{O}_{42}]$. A commercial dry spraying machine (B290, Buchi, Switzerland) was used to prepare micro-spherical $(\text{NH}_4)_{10}[\text{H}_2\text{W}_{12}\text{O}_{42}]$ particles. The impurities of as-synthesized W particles were tested by glow discharge-mass

spectrometry (GD-MS, GD PLUS, ELEMENTTM, Thermo scientific, USA). The phase of solid materials was measured by the X-ray diffraction (XRD, Empyrean, PANalytical, Netherlands, Cu $K\alpha$ radiation at 40 kV). The microstructures of $(\text{NH}_4)_{10}[\text{H}_2\text{W}_{12}\text{O}_{42}]$ and the as-synthesized W particles were observed by scanning electron microscopy (SEM, S-3400N, Hightech, Japan).

2 Results and Discussion

The GD-MS analysis results of raw ammonium paratungstate before and after purification by molybdenum resin and extracting agent are shown in Table 1, where several impurity elements are listed. It can be seen that the purity of the raw ammonium tungstate material is less than 99wt%. After purification by the molybdenum removal resin, the purity is higher than 99.49wt%. We can get that molybdenum resin can efficiently remove the impurities of Mo, Ni and Ba. But many impurities still remain such as Al, Ca and Na. After purification by molybdenum resin and extractant, the purity is higher than 99.99wt%. It is obvious that the composite method has a good effect on removing impurities except calcium. However, compared with the single method, the effect of the composite method on removing calcium is still obvious.

C_0 is the experimental saturation concentration of $(\text{NH}_4)_{10}[\text{H}_2\text{W}_{12}\text{O}_{42}]$ solution at 70 °C, equal to 3.5wt%. Six different solutions, including $1C_0$, $1/2C_0$, $1/4C_0$, $1/8C_0$, $1/16C_0$, $1/32C_0$, were spray dried to be $(\text{NH}_4)_{10}[\text{H}_2\text{W}_{12}\text{O}_{42}]$ particles. The microstructures of as-spray dried $(\text{NH}_4)_{10}[\text{H}_2\text{W}_{12}\text{O}_{42}]$ particles from different concentrations of solution are shown in Fig. 1, in which significantly different morphologies are observed. When the concentration is C_0 , well-dispersed perfect-spherical $(\text{NH}_4)_{10}[\text{H}_2\text{W}_{12}\text{O}_{42}]$ particles are achieved, as can be seen in Fig. 1a. With decreasing the solution concentration, there are some sub-micro pits on the surface of as-spray dried $(\text{NH}_4)_{10}[\text{H}_2\text{W}_{12}\text{O}_{42}]$ particles. By diluting the solution, sub-micro pits on the surface of dried particles increase, as can be seen from Fig. 1b~1d. Interestingly, when the solution concentration is diluted to be very low, the morphology of as-spray dried $(\text{NH}_4)_{10}[\text{H}_2\text{W}_{12}\text{O}_{42}]$ particles is changed to be doughnut (Fig. 1e and Fig. 1f).

The main principle of spray drying process is to deliver and rapidly heat solution via the direct injection of very small droplets. The primary steps include atomization, droplet-to-particle conversion (solvent evaporation), and particle collection. The size and morphology of the final particles produced can be determined by the solution concentration and velocity of the droplet generated by the atomizers^[22,23].

According to the microstructures of the as-spray dried $(\text{NH}_4)_{10}[\text{H}_2\text{W}_{12}\text{O}_{42}]$ particles from different concentrations of solution, evolution process of as-spray dried particles is shown in Fig. 2. Firstly, the $(\text{NH}_4)_{10}[\text{H}_2\text{W}_{12}\text{O}_{42}]$ solution droplets are sprayed to be many fog-drops. And the size of fog-drops should be nearly the same, because the volume of each fog-drop is determined by the volume of droplet and high pressure gas, which are set up the same in this study, i.e., 0.4 mL and 0.6 MPa, respectively. Then, the solvent (water) was evap-

Table 1 Impurities in raw ammonium paratungstate and purified by molybdenum resin and extracting agent (wt%)

Impurity elements	Raw ammonium paratungstate	Purified ammonium paratungstate	
		Purified by molybdenum resin	Purified by molybdenum resin and extracting agent
Na	0.76	0.092	0.0002
Mg	0.13	0.048	<0.0001
Al	0.066	0.18	<0.0001
K	0.042	0.034	0.0005
Ca	0.63	0.11	0.005
Ti	0.009	0.0006	<0.0001
Cr	0.008	0.002	<0.0001
Mn	0.003	0.0007	<0.0001
Fe	0.036	0.013	<0.0001
Ni	0.002	0.0009	<0.0001
Cu	0.013	0.027	0.0002
Zr	0.0004	0.0006	<0.0001
Mo	0.013	0.0007	0.0006
Sn	0.001	0.003	<0.0001
Ba	0.014	0.0008	0.0001
Ta	<0.0001	<0.0001	<0.0001

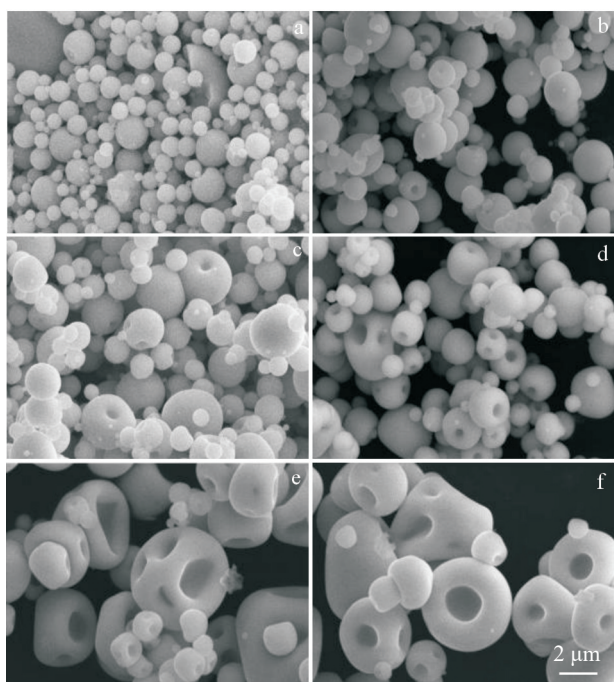


Fig.1 Morphologies of as-synthesized $(\text{NH}_4)_{10}[\text{H}_2\text{W}_{12}\text{O}_{42}]$ powders from different solution concentrations: (a) $1/32C_0$, (b) $1/16C_0$, (c) $1/8C_0$, (d) $1/4C_0$, (e) $1/2C_0$, and (f) $1C_0$

orated in the hot chamber, in which the inlet temperature was $180\text{ }^\circ\text{C}$. As the solvent was evaporated, the solute $(\text{NH}_4)_{10}[\text{H}_2\text{W}_{12}\text{O}_{42}]$ was separated out to be solid phase on the surface of for-drop. After that, separated $(\text{NH}_4)_{10}[\text{H}_2\text{W}_{12}\text{O}_{42}]$ was aggregated to be shell. However, the thickness of the shell was de-

pendent on the concentration, that is, low concentration equals to thin shell, while high concentration corresponds to thick shell.

When the solution concentration is low, such as $1/32C_0$ and $1/16C_0$, thin shell forms after the evaporation. The thin shell is too weak to prevent the crash from other particles. So there are many sub-micro pits on the particles' surface, and even the morphology is changed to be doughnut. However, when the solution is high (C_0), shell is thick and strange enough to resist the collision from other particles. So the perfect-micro-spherical $(\text{NH}_4)_{10}[\text{H}_2\text{W}_{12}\text{O}_{42}]$ particles are obtained. Thus, the final morphology of as-spray dried $(\text{NH}_4)_{10}[\text{H}_2\text{W}_{12}\text{O}_{42}]$ particles are determined by the solution concentration.

The relationship between calcination temperature and particles' morphology and size was studied, in order to search the particle growth situation during the calcination process in high purity N_2/H_2 atmosphere. And the principle of ammonium paratungstate thermal decomposition was obtained by Ref. [24-26].

When the temperature was lower than $200\text{ }^\circ\text{C}$, ammonium paratungstate will slightly decompose, removing a small amount of crystal water and ammonium ions but still maintaining its basic structure. In the temperature range of $200\sim 300\text{ }^\circ\text{C}$, all crystal water and large part of ammonium ions are removed. When the temperature is between $300\sim 350\text{ }^\circ\text{C}$, great phase transition occurs, forming metastable tungsten oxide species (WO_x). When the temperature is raised above $350\text{ }^\circ\text{C}$, the metastable tungsten oxide species are transformed to WO_3 . When the temperature reaches $600\text{ }^\circ\text{C}$, WO_x is converted to

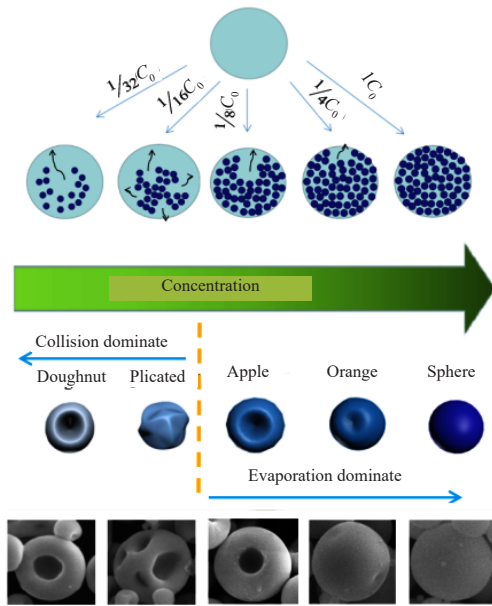
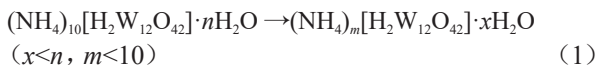


Fig.2 Schematic diagram of particle morphology as a function of initial solution concentration

WO₂. And as the temperature reaches 650 °C, WO₂ is reduced to W. With the gradual increase of temperature, all WO₂ is reduced to W, as shown in Eq.(1)~Eq.(6).

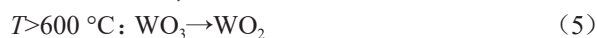
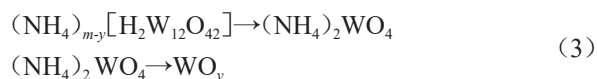
$T < 200\text{ }^{\circ}\text{C}$:



$200\text{ }^{\circ}\text{C} < T < 300\text{ }^{\circ}\text{C}$:



$300\text{ }^{\circ}\text{C} < T < 350\text{ }^{\circ}\text{C}$:



XRD patterns of tungsten powders pyrolyzed at different temperatures (600, 650, 700 and 750 °C) in N₂/H₂ (v/v 3:1) atmosphere for 2 h are shown in Fig.3. After calcination at 600 °C in N₂/H₂ for 2 h, the as-spray dried (NH₄)₂WO₄ powders completely decompose and transform to WO₂ powder. When the temperature increases to 650 °C, part of WO₂ is reduced to W. When the temperature is 700 °C, WO₂ is reduced to W completely, and good crystallization can be observed. The W powder, obtained by spray dried (NH₄)₂WO₄ particles reduced at 750 °C, also shows good crystallization (green line in Fig.3), while the XRD peaks are much weaker and wider than the XRD peaks of 700 °C. It is indicated that W powder is recrystallized at 750 °C.

The morphologies of as-synthesized W particles at different calcination temperatures are shown in the Fig.4. As the temperature increases, the particles maintain a basic shape at 600 °C, and the particle size distribution ranges from 0.5 μm to 4 μm with an average size about 2 μm (as shown in Fig.4a).

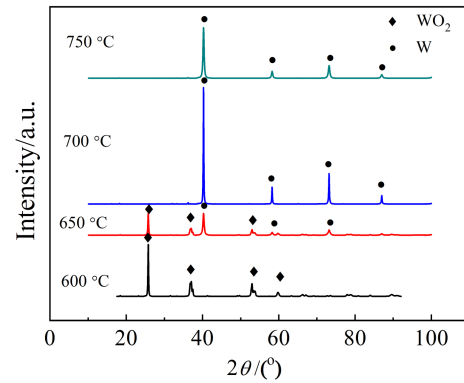


Fig.3 XRD patterns of tungsten powder after sintering at different temperatures

Corresponding to the XRD results (black line in Fig.3), the particle composition is WO₂. As the temperature increases to 650 °C, WO₂ is reduced to W, and the overall morphology of the particles and size remain basically unchanged (as shown in Fig.4b). When the temperature is raised to 700 °C and held for 2 h (Fig.4c), a large amount of WO₂ is reduced, which causes the particles to break apart from the original position. When the temperature reaches 750 °C, as shown in Fig.4d, the sublimation of WO₂ is suppressed and the hydrogen reduction performance is very strong, leading to rapid reduction of WO₂ without changing the overall morphology of the particles. However, primary particles grow up due to high temperature, and the size distribution of as-prepared W particles is between 1 μm and 6 μm, and the average size is about 3 μm.

Two-step calcination process is carried out for the investigation of W particle growth mechanism. As-spray dried (NH₄)₁₀[H₂W₁₂O₄₂] particles were calcined at 700 °C for 2 h, and then raised to 750 °C for 2 h. The morphologies of two-step as-calcined W particles is shown in Fig.5. After calcination at 700 °C for 2 h, all the tungsten oxide can be reduced, so the morphology is fixed. By continuous calcination at 750 °C for 2 h, W particles get the energy to aggregation (particle to particle). Thus, the particle size of as-prepared W by two-step calcination is bigger than at 700 °C calcination, but smaller than at 750 °C calcination.

The microstructural transformation mechanism of spray dried (NH₄)₁₀[H₂W₁₂O₄₂] particles during thermal decomposition is revealed in Fig.6. With increasing the temperature, the particles keep their basic shape at 600 °C. The grains are very small, and the particle composition is WO₂. By raising temperature to 650 °C, part of WO₂ is reduced to W by H₂, while particle morphology and size are basically unchanged. When the temperature is increased to 700 °C and kept for 2 h, most of WO₂ is reduced, for which the particles are deviated from their original positions, resulting in the particle breakage. Because of the increase of temperature, the primary particles grow up. When the temperature reaches 750 °C, the sublimation of WO₂ is restrained. Meanwhile, the reduction performance of hydrogen is very strong, which cause the rapid reduction of WO₂ and basically unchanged overall morphology of the particles.

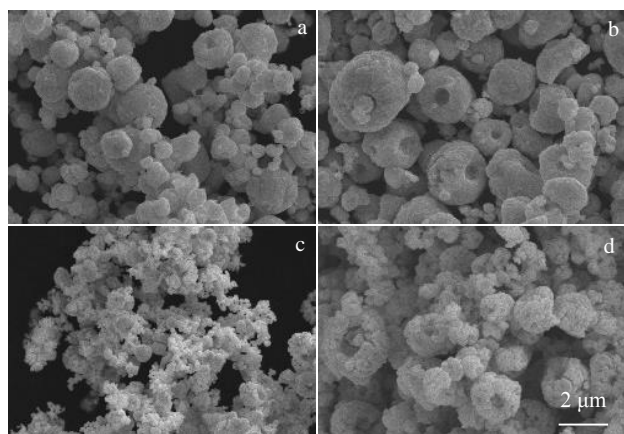


Fig.4 SEM morphologies of spray-dried ammonium tungsten at different calcination temperatures: (a) 600 °C, (b) 650 °C, (c) 700 °C, and (d) 750 °C

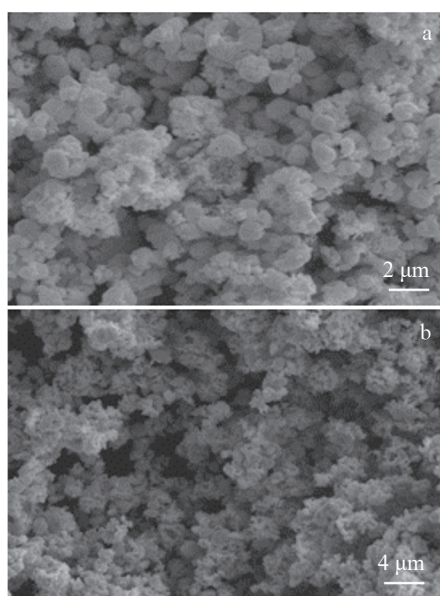


Fig.5 SEM morphologies of spray-dried ammonium tungsten at room temperature and after secondary calcination at different multiples

Two-step pyrolysis shows different results from the one-step pyrolysis, as can be seen on the right side of Fig.6. As-spray dried $(\text{NH}_4)_{10}[\text{H}_2\text{W}_{12}\text{O}_{42}]$ particles are broken due to the sublimation of WO_2 during the 1st 700 °C pyrolysis treatment. And the as-pyrolyzed broken W particles are aggregated again in the 2nd 750 °C pyrolysis treatment. Thus, the final as-pyrolyzed W particles treated by two-step pyrolysis are kindly broken particles, while the particles' size is larger than that of one-step pyrolysis (750 °C) treated particles.

3 Conclusions

1) High-purity (99.995wt%) well-dispersed micro-spherical W particles can be prepared from crude ammonium tungstate by hydrometallurgy and spray dry-pyrolysis process. The impurities in crude ammonium tungstate, including Mo, Na, Fe, Al, etc, are effectively eliminated by the ion exchange and

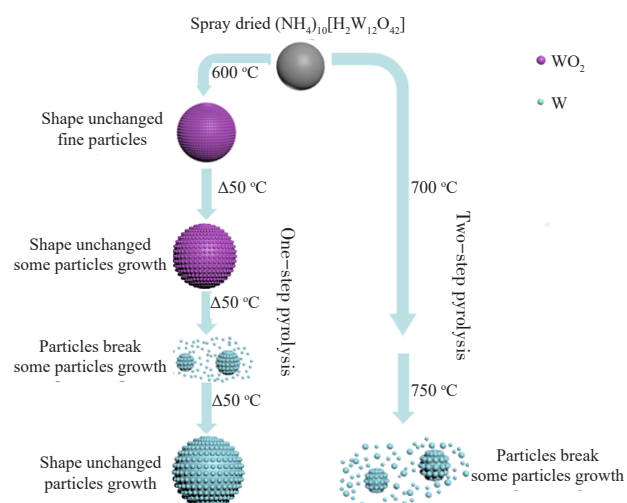


Fig.6 Microstructural transformation mechanisms of spray dried $(\text{NH}_4)_{10}[\text{H}_2\text{W}_{12}\text{O}_{42}]$ particles during thermal decomposition

extraction treatments.

2) The morphology of as-spray dried $(\text{NH}_4)_{10}[\text{H}_2\text{W}_{12}\text{O}_{42}]$ particles is influenced by the solution concentration. By spray drying the dilute solution (1/32 C_0), doughnut $(\text{NH}_4)_{10}[\text{H}_2\text{W}_{12}\text{O}_{42}]$ particles are obtained, while perfect spherical $(\text{NH}_4)_{10}[\text{H}_2\text{W}_{12}\text{O}_{42}]$ particles are achieved by spray dried saturated solution.

3) Pyrolysis temperature is one of key factors for controlling the morphology and size of as-prepared W particles. Well-dispersed micro-spherical W particles can be obtained by pyrolysis at 750 °C.

References

- Fan J, Han Y, Li P et al. *Journal of Nuclear Materials*[J], 2014, 455: 717
- Trunev Yu A, Arakcheev A S, Burdakov A V et al. *AIP Conference Proceedings*[J], 1771: 60 016
- Lin J W, Chang H C, Wu M H. *Journal of Manufacturing Processes*[J], 2014, 16: 296
- Sato K, Nakamura K, Suzuki S et al. *Fusion Technology*[J], 1996, 30: 769
- Yu Y, Song J, Bai F et al. *International Journal of Refractory Metals and Hard Materials*[J], 2015, 53: 98
- Findik F, Uzun H. *Materials & Design*[J], 2003, 24(7): 489
- Kamal S S K Sahoo, Vimala P K, Shanker B J et al. *Journal of Alloys and Compounds*[J], 2019, 678: 403
- Ren C, Fang Z Z, Zhang H et al. *International Journal of Refractory Metals and Hard Materials*[J], 2016, 61: 273
- Jung J C, Ko S G, Won C W et al. *Journal of Materials Research* [J], 1996, 11(7): 1825
- Green T E. *Analytical Chemistry* [J], 1965, 37(12): 1595
- Sun Peimei, Chen houxi, Li Honggui et al. *Journal of Central South University of Technology*[J], 1996, 3(2): 171
- Macinnis M B, Kim T K. *Journal of Chemical Technology and*

- Biotechnology*[J], 1979, 29(4): 225
- 13 Prestigiacomo M, Bedu F, Jandard F et al. *Applied Physics Letters*[J], 2005, 86(19): 192-112
- 14 Long Luping, Liu Wensheng, Ma Yunzhu et al. *High Temperature Materials and Processes*[J], 2015, 34(6): 605
- 15 Zhao Panchao, Yi Wei, Cao Qigao et al. *Nanoscale Res Lett*[J], 2019, 14(1): 68
- 16 Zhao Qinsheng. *Journal Rare Metals and Cemented Carbides* [J], 2003, 31(4): 56
- 17 Okuyama K, Wuled Lenggoro I. *Chemical Engineering Science* [J], 2003, 58(3-6): 537
- 18 Venil C K, Khasim A R, Aruldass C A et al. *International Bio-deterioration & Biodegradation*[J], 2016, 113: 350
- 19 Bustamante M, Oomah B D, Rubilar M et al. *Food Chemistry* [J], 2017, 216: 97
- 20 Bi J, Yi W, Chen J et al. *Advanced Powder Technology*[J], 2016, 27(1): 53
- 21 Kalpakli A O, Arabaci A, Kahruman C et al. *International Journal of Refractory Metals and Hard Materials*[J], 2013, 37: 106
- 22 Iskandar F. *Adv Powder Tech*[J], 2009, 20(4): 283
- 23 Nandiyanto A B D, Okuyama K. *Adv Powder Tech*[J], 2011, 22 (1): 1
- 24 French G J, Sale F R. *Journal of Materials Science*[J], 1981, 16 (12): 3427
- 25 Basu A K, Sale F R. *Journal of Materials Science*[J], 1977, 12 (6): 1115-1124
- 26 van Put J W. *International Journal of Refractory Metals and Hard Materials*[J], 1995, 13(1-3): 61

湿法冶金结合喷雾干燥-热解工艺纯化和控制钨颗粒

李安金¹, 赵盘巢², 易伟¹, 辛泽娜¹, 李鸿鹏¹, 逢芳钊¹, 李继刚¹, 姚陈思琪¹

(1. 昆明贵金属研究所 稀贵金属材料综合利用先进技术国家重点实验室, 云南 昆明 650106)

(2. 西北有色金属研究院, 陕西 西安 710016)

摘要: 钨因其独特的物理化学性能而被广泛的应用于半导体和高温材料。依次采用离子交换、溶剂萃取、重结晶、喷雾干燥和煅烧还原的方法对钨酸铵进行处理, 成功制备出高纯、分散性好的微米级球形钨粉。其中, 利用湿法冶金去除原料中的杂质金属, 喷雾干燥和煅烧还原过程控制最终钨粉形貌结构和粒径分布。研究了喷雾干燥过程中溶液浓度对雾化粉末形貌的影响规律, 并揭示了雾化粉末分解还原过程中的机理。结果表明, 该方法制备出的钨粉纯度高于99.995%, 平均尺寸约为1.5 μm。本研究中的湿法冶金和粉末技术可用于合成其它具有高性能要求的金属粉末。

关键词: 高纯度; 分散性良好; 微球形; 溶液浓度; 热解机理

作者简介: 李安金, 男, 1995年生, 硕士生, 昆明贵金属研究所稀贵金属材料综合利用先进技术国家重点实验室, 云南 昆明 650106, E-mail: 422309642@qq.com